

Synthesizing Nonstoichiometric $\text{Li}_{3-3x}\text{V}_{2+x}(\text{PO}_4)_3/\text{C}$ as Cathode Materials for High-performance Lithium-ion Batteries by Solid State Reaction

Pingping Sun ¹, Ningang Su ¹, Yuanting Wang ¹, Qingyu Xu ^{1,2*}, Qi Fan ^{3*}, Yueming Sun³

¹ Department of Physics, Southeast University, Nanjing 211189, China

² National Laboratory of Solid State Microstructures, Nanjing University, Nanjing 210093, China

³ College of Chemistry and Chemical Engineering, Southeast University, Nanjing 211189, China

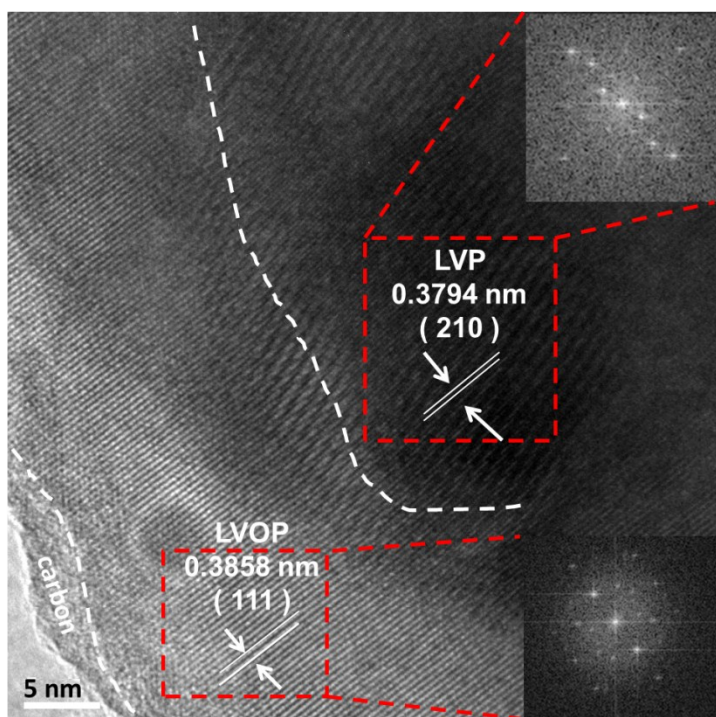


Fig. S1 HRTEM image of LVP-0.10.

A typical HRTEM image (Fig. S1) is presented to investigate the structure of LVP-0.10. Two types of lattice fringes are found in the composites: the $\text{Li}_3\text{V}_2(\text{PO}_4)_3$ lattice

fringe with an interplanar spacing of 0.3794 nm that corresponds to the (210) lattice planes; and the LiVOPO_4 lattice fringe with an interplanar spacing of 0.3858 nm that corresponds to the (111) lattice planes. Fast Fourier transform (FFT) was performed in the selected crystal planes to confirm the different phases, as shown in inset. The FFT images of the selected regions show the diffraction patterns of $\text{Li}_3\text{V}_2(\text{PO}_4)_3$ and LiVOPO_4 , respectively. Different diffraction patterns are obtained, indicating that two phases coexist in the samples. The HRTEM image confirms the $\text{Li}_3\text{V}_2(\text{PO}_4)_3$ core and LiVOPO_4 shell structure, similar to our previous report. [1]

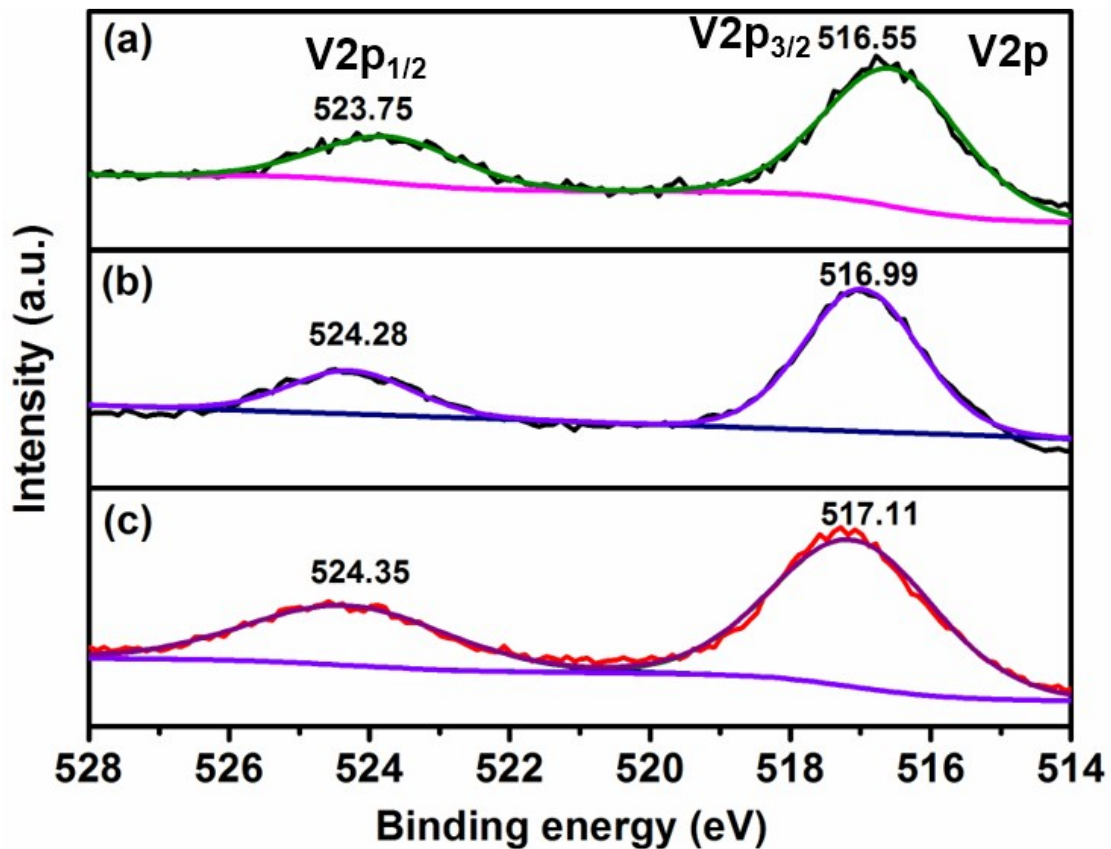


Fig. S2 V2p XPS spectra of LVP-0.10 prepared by (a) sol-gel, (b) sol-gel + ball mill, (c) solid state reaction.

XPS is provided to detect the surface phase. V2p peaks of LVP-0.10 (Fig. S2) prepared by solid state reaction significantly shifts to higher binding energy, compared with that prepared by sol-gel method [2] and is close to that prepared by sol-gel with ball mill method [1]. The binding energies are consistent with those of V^{4+} in LiVOPO_4 .

Table S1. The comparison of electrochemical performance among $\text{Li}_3\text{V}_2(\text{PO}_4)_3$ nanocomposites.

Active Nanomaterials	10C	20C	Cycle Number	References
	Specific Capacity(mAh/g) 3-4.3V before (after cycles)			
Hierarchical $\text{Li}_3\text{V}_2(\text{PO}_4)_3/\text{C}$ Mesoporous Nanowires	117	/	/	3
$\text{Li}_3\text{V}_2(\text{PO}_4)_3$ /PEDOT composite	122(122)	/	100	4
$\text{Li}_3\text{V}_2(\text{PO}_4)_3$ 3D Foams	112	105		5
Ionic-Liquid-Assisted Synthesis $\text{Li}_3\text{V}_2(\text{PO}_4)_3$	108(102.6)	105(100)	100	6
Hierarchical Carbon Decorated $\text{Li}_3\text{V}_2(\text{PO}_4)_3$	123	122(94)	4000	7
$\text{Li}_3\text{V}_2(\text{PO}_4)_3$ /graphene nanocomposites	/	109(108)	100	8
core-shell structured $\text{Li}_3\text{V}_2(\text{PO}_4)_3@\text{C}$	97.9(107.8)	/	300	9
LVP/C + RuO_2	102.5(101)	/	100	10
Sol-gel synthesized $\text{Li}_{3-3x}\text{V}_{2+x}(\text{PO}_4)_3/\text{C}$	126	92.5	85.1	2
Core-shell-structured $\text{Li}_3\text{V}_2(\text{PO}_4)_3\text{-LiVOPO}_4$ nanocomposites	121.5	116.3(111)	1000	1
Solid state reaction synthesized $\text{Li}_{3-3x}\text{V}_{2+x}(\text{PO}_4)_3/\text{C}$	124.6	124.3(122.2)	1000	This work

Table S2. The comparison of electrochemical performance among $\text{Li}_3\text{V}_2(\text{PO}_4)_3$ nanocomposites made by different methods.

Method	10C	20C	Cycle Number	References
	Specific Capacity(mAh/g) 3-4.3V before (after cycles)			
Sol-gel	126	92.5	85.1	2
Sol-gel + ball mill	121.5	116.3(111)	1000	1
Ball mill	124.6	124.3(122.2)	1000	This work

Table S3. The comparison of electrochemical kinetic parameters among $\text{Li}_3\text{V}_2(\text{PO}_4)_3$ nanocomposites prepared by different methods.

Method	Li diffusion coefficient D_{Li^+} ($\text{cm}^2 \text{s}^{-1}$)	Electron conductivity σ_e (S cm^{-1})	Charge transfer resistance R_{ct} (Ω)	Reference
Sol-gel	1.45×10^{-9}	9.54×10^{-5}	92.7	2
Sol-gel+ball mill	1.04×10^{-9}	1.77×10^{-4}	50	1
Ball mill	1.84×10^{-9}	1.42×10^{-4}	62.4	This work

References

- [1] P. Sun, X. Wang, K. Zhu, X. Chen, X. Cui, Q. Xu, D. Su, Q. Fan, Y. Sun, *RSC Adv.*, 2017, **7**, 3101–3107.
- [2] P. Sun, S. Qin, X. Wang, R. An, Q. Xu, X. Cui, Y. Sun, S. Wang, P. Wang, Q. Fan, *J. Power Sources*, 2015, **293**, 922–928.
- [3] Q. Wei, Q. An, D. Chen, L. Mai, S. Chen, Y. Zhao, K.M. Hercule, L. Xu, A. Minhas-Khan, Q. Zhang, *Nano Lett.*, 2014, **14**, 1042–1048.
- [4] J. Kim, J.K. Yoo, Y.S. Jung, K. Kang, *Adv. Energy Mater.*, 2013, **3**, 1004–1007.
- [5] Y. Zhou, X. Rui, W. Sun, Z. Xu, Y. Zhou, W.J. Ng, Q. Yan, E. Fong, *ACS Nano*, 2015, **9**, 4628–4635.
- [6] X. Zhang, N. Bçckenfeld, F. Berkemeier, A. Balducci, *ChemSusChem*, 2014, **7**, 1710–1718.
- [7] Y. Luo, X. Xu, Y. Zhang, Y. Pi, Y. Zhao, X. Tian, Q. An, Q. Wei, L. Mai, *Adv. Energy Mater.* 2014, **1400107**, 1-8.

- [8] H. Liu, P. Gao, J. Fang, G. Yang, *Chem. Commun.*, 2011, **47**, 9110–9112.
- [9] C. Wang, H. Liu, W. Yang, *J. Mater. Chem.*, 2012, **22**, 5281–5285.
- [10] R. Zhang, Y. Zhang, K. Zhu, F. Du, Q. Fu, X. Yang, Y. Wang, X. Bie, G. Chen, Y. Wei, *ACS Appl. Mater. Interfaces*, 2014, **6**, 12523–12530.